

Supporting information

I. Experimental section

Due to moisture and air sensitivity, all utilized metals, intermetallics and hydrides were handled in an argon-filled glove box. The alloys $\text{LiEu}_x\text{M}_{1-x}$ ($\text{M} = \text{Sr, Ba}$) were prepared by melting reactions of the elements (Eu ingots, Alfa Aesar, 99.9%; strontium pieces, Alfa Aesar, 99.8%; barium rod, Chempur, 99.3% (rest strontium); lithium wire, Alfa Aesar, 99.8%, all mechanically surface cleaned before use) in Nb ampoules and hydrogenated in an autoclave consisting of the hydrogen resistant *Nicrofer®* 5219 alloy (Inconel 718) at approx. 600K and hydrogen (Praxair, 99.9%) or deuterium (Praxair, 99.8%) pressure of 70-180 bar.

II. Characterization

X-ray powder diffraction data were collected on a Panalytical Philips *X'Pert Pro* diffractometer with focusing Bragg-Brentano geometry and a fine focus X-ray tube ($\text{CuK}\alpha_{1,2}$ radiation). Samples were enclosed between kapton foils with apiezon grease. The data collection time was 60 min, diffraction range $10 - 110^\circ 2\theta$, below $22^\circ 2\theta$ an increased amorphous background occurred due to sample preparation. Crystal structures were refined via Rietveld analysis using TOPAS 4.2 (Bruker AXS, Karlsruhe, Germany)¹ and the fundamental parameter approach². The instrumental function was determined empirically by means of a reference scan of LaB_6 . Typically, complete structures including hydrogen positions from literature were taken as starting structures and scale factors, lattice parameters, atomic positions of the metal atoms and microstructural parameters were refined. Standard deviations in the lattice constants are given as calculated by the program TOPAS4.2. It should be noted that Rietveld refinement programs usually tend to underestimate such standard deviations³.

Neutron powder diffraction data were collected at the high-flux diffractometer D20 at the Institute Laue-Langevin (Grenoble, France) in high resolution mode with total data collection times of 20 minutes each. Samples were enclosed in vanadium cylinders sealed by an indium wire and handled in an argon-filled glove-box. Structural refinement was carried out with TOPAS 4.2 using both the XRD and neutron data. The same positional and size and strain parameters were used. The instrumental function for the neutron data was determined empirically by means of a reference scan of a Si standard (NIST640b), which yielded the actual neutron wavelength 186.630(2) pm. Neutron data clearly showed that the compounds crystallize in the inverse cubic perovskite type. (LiSrH_3 Rwp (obtained using TOPAS4.2) inverse model 2.84, normal model 8.18; LiBaH_3 Rwp inverse model 3.33, normal model 20.87)

Small amounts of the corresponding alkaline earth metal hydrides were present; this should, however, not cause problems observing Eu(II)-luminescence in the main phase, as the Eu(II) luminescence in alkaline earth metal hydrides is known and of weak intensity⁴.

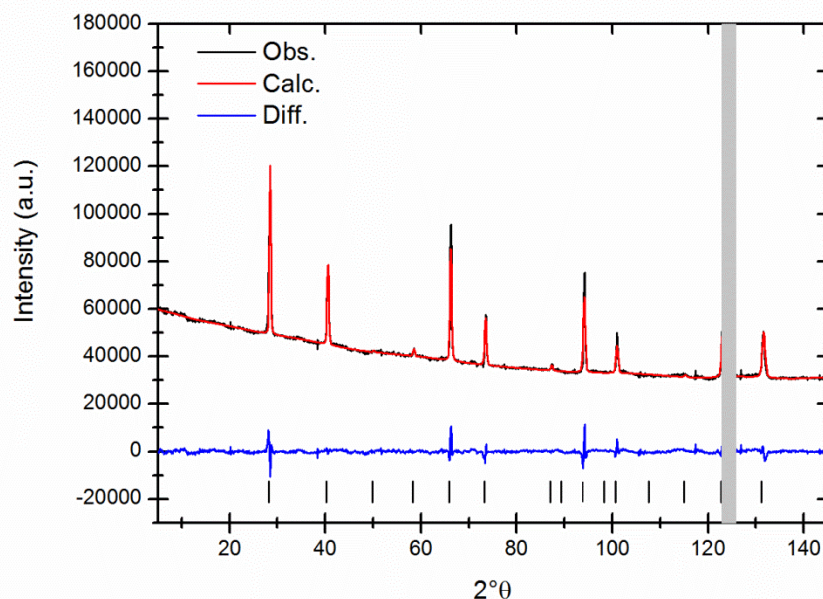


Figure 1: Rietveld analysis of the neutron powder diffraction data of LiSrH_3 .

Further luminescence spectra not given in the main article are depicted below.

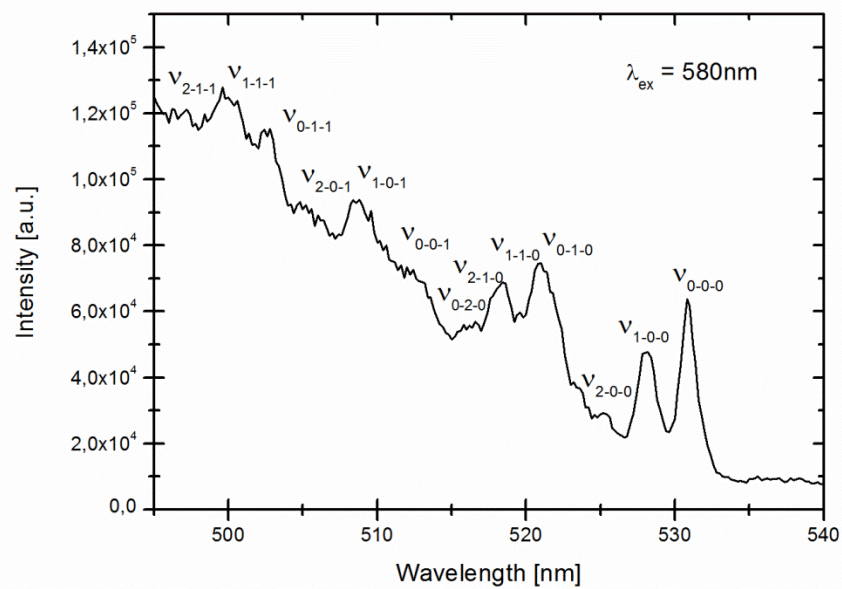


Figure 2: Details in the excitation spectrum of $\text{LiSrH}_3:\text{Eu}^{2+}$ (0.5%) at 4 K, emission at 580 nm.

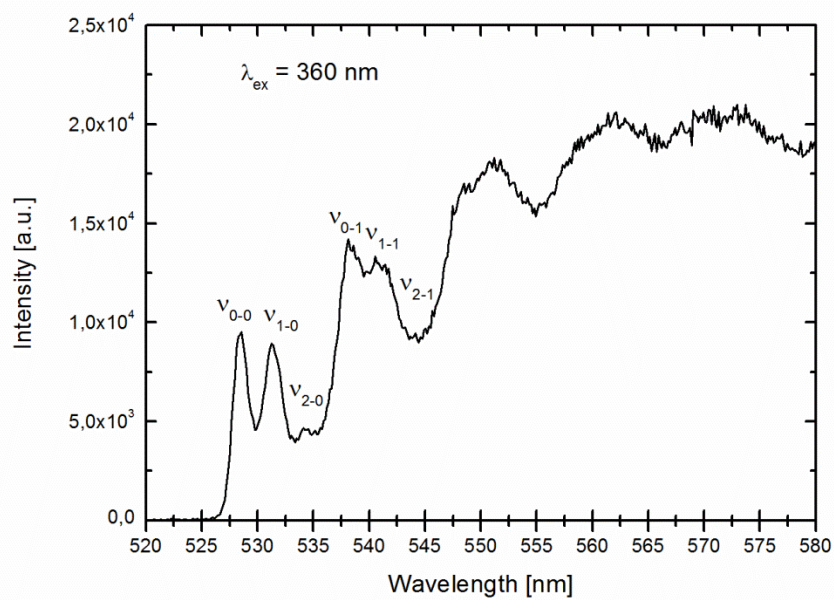


Figure 3: Details in the emission spectrum of $\text{LiSrD}_3:\text{Eu}^{2+}$ (0.5%) at 4K, excitation at 360 nm.

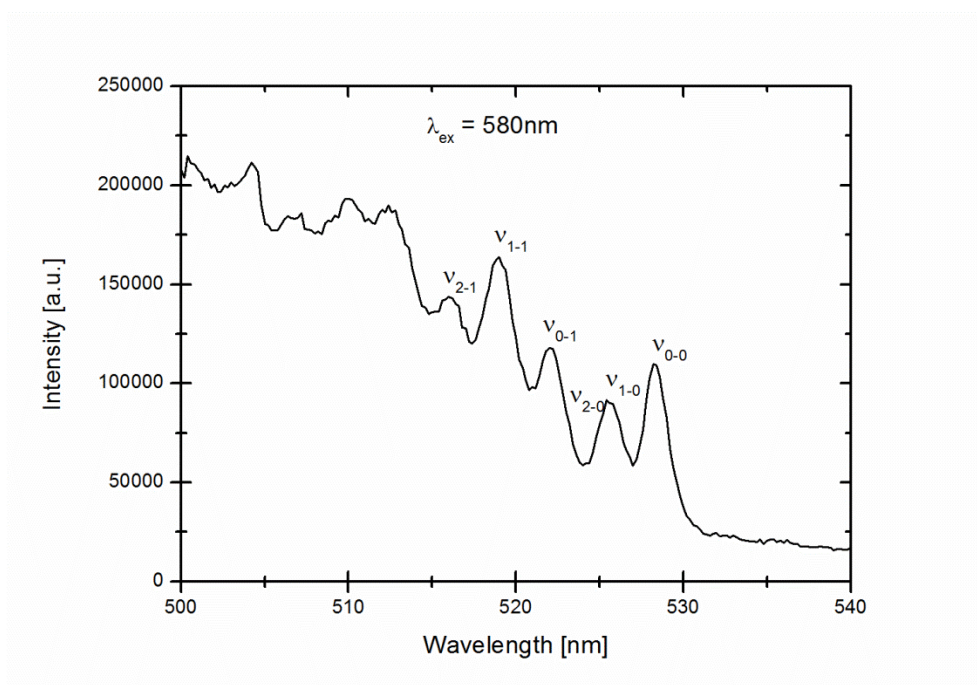


Figure 4: Details in the excitation spectrum of $\text{LiSrD}_3:\text{Eu}^{2+}$ (0.5%) at 4K, emission at 580 nm.

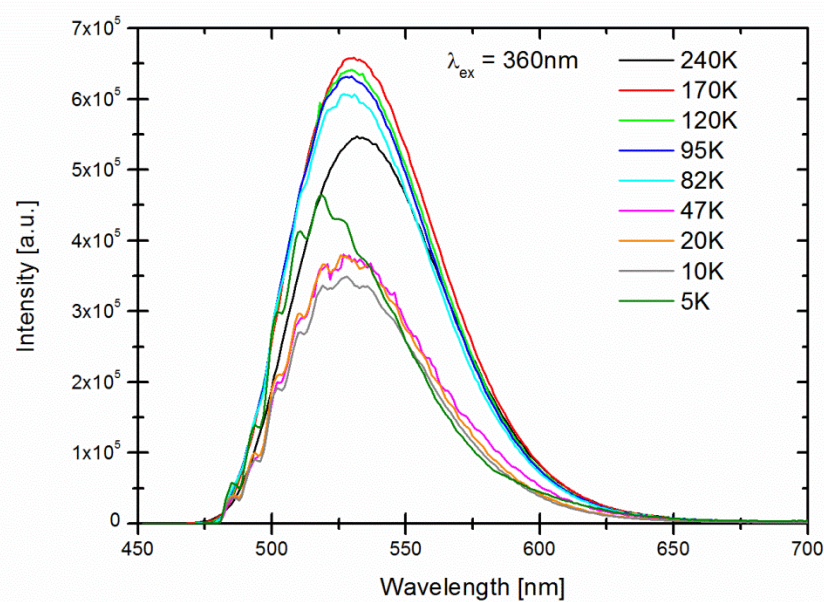


Figure 5: Temperature-dependent luminescence spectra of $\text{LiBaD}_3:\text{Eu}^{2+}$ (0.5%).

Table 1. Vibronics in the excitation and emission spectrum at 5 K for the $4f^65d - ^8S_{7/2}$ transition of Eu²⁺ in LiBaH₃:Eu²⁺ and LiBaD₃:Eu²⁺ (0.5 mol%). ΔE gives the energy of the vibrational modes with respect to their zero phonon lines.

Emission	Excitation				
	LiBaH ₃ :Eu ²⁺	LiBaD ₃ :Eu ²⁺	Line	LiBaH ₃ :Eu ²⁺	LiBaD ₃ :Eu ²⁺
Line	ΔE [cm ⁻¹]	ΔE [cm ⁻¹]	Line	ΔE [cm ⁻¹]	ΔE [cm ⁻¹]
ν_1	89	103	ν_1	77	86
ν_2	164	188	ν_2	128	178

Luminescence decay curves were analyzed using a single exponential function, even though the curves in the higher temperature range for the partly quenched luminescence were not perfectly single exponential. An example for a decay curve is given in Fig.5.

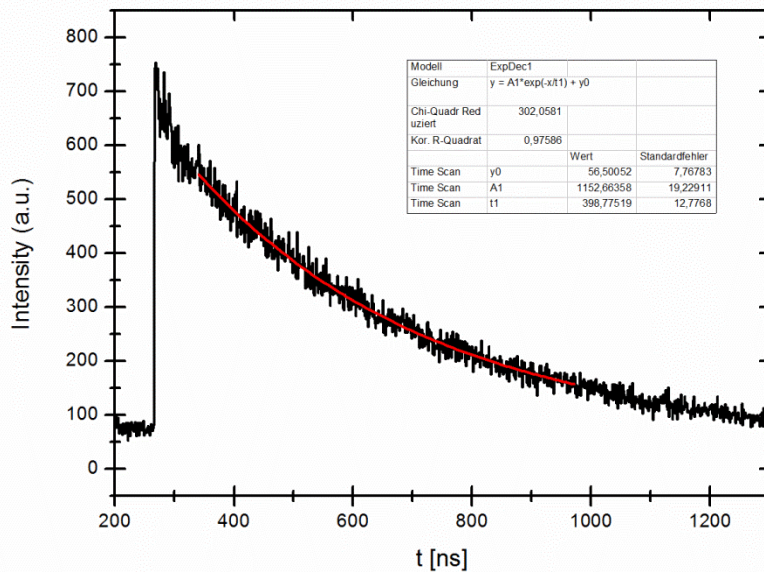


Figure 6: Decay curve at 42 K of LiSrH₃:Eu²⁺, emission at 580 nm.

1 Bruker AXS, Karlsruhe, TOPAS V4.2, *General profile and structure analysis software for powder diffraction data, Users's Manual*, (2009).

2 Coelho, A. A 2003 *J. Appl. Crystallogr.* **36**, 86-95.

3 Toby, B. H. 2006 *Powder Diffr.* **21**, 67-70.

4 Kunkel, N.; Kohlmann, H.; Sayede, A.; Springborg M. 2011 *Inorg. Chem.* **50**, 5873-5875.